

Evidence of topological insulator state in LaBi semimetal

R. Lou,¹ B.-B. Fu,² Q. N. Xu,² P.-J. Guo,¹ L.-Y. Kong,² L.-K. Zeng,² J.-Z. Ma,² P. Richard,^{2,3,4} C. Fang,² Y.-B. Huang,⁵ S.-S. Sun,¹ Q. Wang,¹ L. Wang,² Y.-G. Shi,² H. C. Lei,¹ K. Liu,¹ H. M. Weng,^{2,4} T. Qian,^{2,4} H. Ding,^{2,3,4} and S.-C. Wang^{1,*}

¹Department of Physics and Beijing Key Laboratory of Opto-electronic Functional Materials & Micro-nano Devices, Renmin University of China, Beijing 100872, China

²Beijing National Laboratory for Condensed Matter Physics, and Institute of Physics, Chinese Academy of Sciences, Beijing 100190, China

³School of Physical Sciences, University of Chinese Academy of Sciences, Beijing 100190, China

⁴Collaborative Innovation Center of Quantum Matter, Beijing, China

⁵Shanghai Synchrotron Radiation Facility, Shanghai Institute of Applied Physics, Chinese Academy of Sciences, Shanghai 201204, China

By employing angle-resolved photoemission spectroscopy combined with first-principles calculations, we performed a systematic investigation on the electronic structure of LaBi, which exhibits extremely large magnetoresistance (XMR), and is theoretically predicted to possess band anti-crossing with nontrivial topological properties. Here, the observation of the Fermi surface topology and band dispersions are similar to previous studies on LaSb [Phys. Rev. Lett. **117**, 127204 (2016)], a topologically trivial XMR semimetal, except the existence of a band inversion along the Γ -X direction, with one massless and one gapped Dirac-like surface states at the X and Γ points, respectively. The odd number of massless Dirac cones suggests that LaBi is analogous to the time-reversal Z_2 nontrivial topological insulator. These findings open up a brand-new series for exploring novel topological states and investigating their evolution from the perspective of topological phase transition within the family of rare earth monpnictides.

PACS numbers: 73.20.At, 71.18.+y, 79.60.-i, 71.20.Eh

Exploring exotic topological states has sparked extensive research interest, both theoretically and experimentally, as their promising potential in low consumption spintronics devices¹⁻³. In the past decade, since the discovery of quantum spin Hall effect in graphene⁴, remarkable achievements have been reached, including the findings of two-dimensional (2D)⁵⁻⁷ and three-dimensional (3D) topological insulators (TIs)⁸, node-line semimetals^{9,10}, topological crystalline insulators^{11,12}, Dirac and Weyl semimetals¹³⁻¹⁸. Strikingly, although the TIs have ignited the whole field for years, the realization of novel massless surface Dirac fermions, *i.e.*, topological surface states (SSs), is still pretty exciting due to the great prospects in tunability of the topological characteristics through easily accessible manipulations¹⁹. Among the extensive efforts, the study on the topological phase transition (TPT) can also effectively facilitate the exploration and investigation of topological SSs and even the Dirac semimetals²⁰⁻²².

Recently, the discovery of simple rock salt rare earth monpnictides LnX (Ln = La, Y, Nd, or Ce, X = Sb/Bi)²³⁻²⁹ has renewed the platform for searching these novel topological states. The most remarkable signature of this series is the extremely large magnetoresistance (XMR) with a resistivity plateau at low temperatures, which is proposed as the consequence of breaking time reversal symmetry²³. However, the theoretical predictions for the topological properties vary in the LnX series³⁰. In addition, similar fingerprints have also been reported in several semimetals including TmPn₂ (Tm = Ta/Nb, Pn = As/Sb)³¹⁻³⁶, ZrSiS³⁷⁻³⁹, WTe₂⁴⁰, Cd₃As₂^{41,42}, TaAs⁴³, and NbP⁴⁴. The topological origin of the large magnetoresistance and resistivity plateau is still under debate. Furthermore, the rich and interesting topological phases predicted in the LnX family offer an unprecedented opportunity for in-

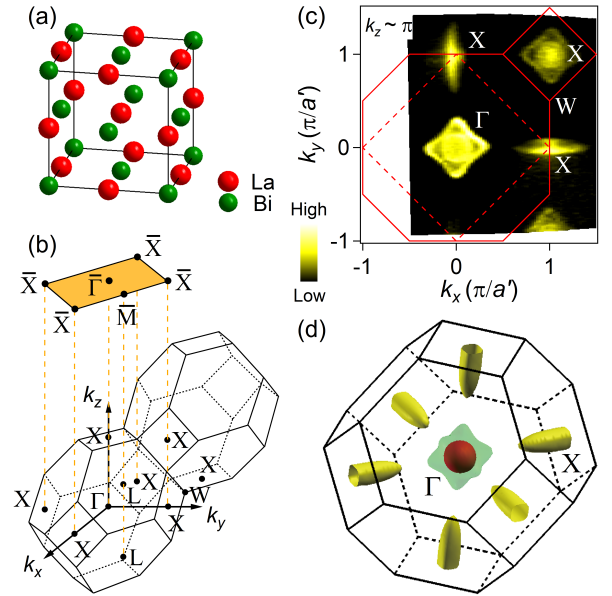


FIG. 1: (Color online) Crystal structure and FS topologies of LaBi. (a) Crystal structure of LaBi. (b) Bulk BZ and the (001)-projected surface BZ of LaBi. (c) FS intensity plot of LaBi recorded with $h\nu = 84$ eV, corresponding to the $k_z \sim \pi$ plane, obtained by integrating the spectral weight within ± 10 meV with respect to E_F . a' is the half of the lattice constant a of the face-center-cubic unit cell. Red solid and dashed lines represent the 3D BZ and 2D surface BZ, respectively. (d) Calculated 3D FSs using the PBE functional.

vestigating the novel topological properties and TPT in a relatively simple system without convoluted bulk and SSs^{30,45-48}. To our knowledge, although there have been several angle-

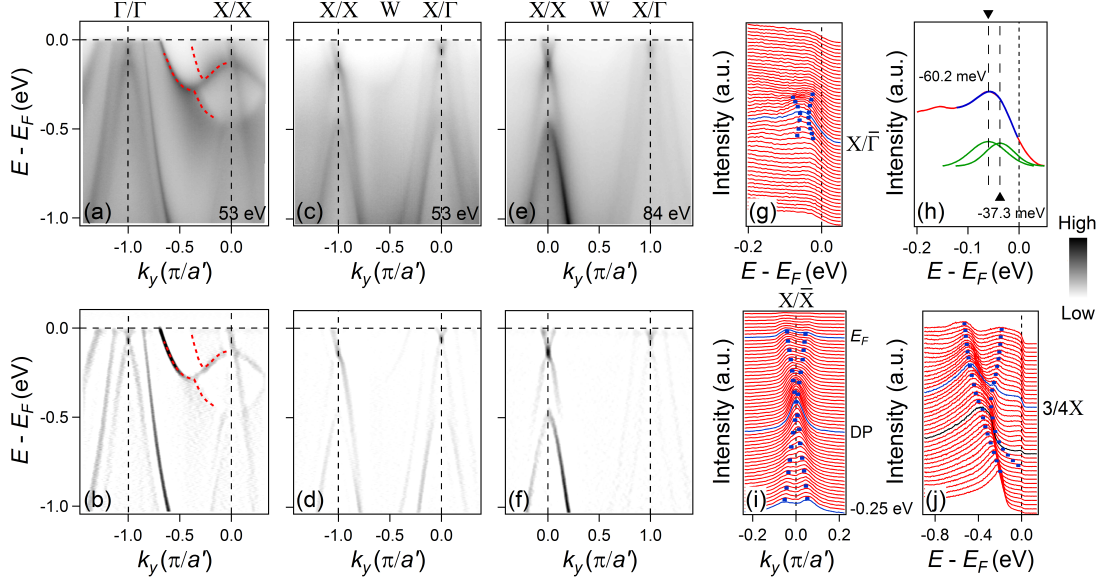


FIG. 2: (Color online) Band dispersions along high-symmetry lines taken at the $k_z \sim 0$ ($h\nu = 53$ eV) and $k_z \sim \pi$ ($h\nu = 84$ eV) planes of LaBi. (a),(b) Photoemission intensity plot along the Γ -X direction and corresponding second derivative plot recorded with $h\nu = 53$ eV, respectively. Red dashed curves are guides to the eye for the band anti-crossing feature. (c),(d) Same as (a),(b) but along the X-W-X directions. (e),(f) Same as (c),(d) but measured with $h\nu = 84$ eV, displaying more prominent surface band features around the left X point. (g) EDC plot of (e) around the right X point. (h) Single EDC at the right X point in (e), highlighted by blue curve in (g). By fitting the EDC with two Lorentzian profiles, shown as green curves, we extract the peak positions, marked by two vertical dashed lines, and determine the presence of a surface band gap of ~ 23 meV. The blue curve is the superimposed fitting result. (i) MDC plot of (e) around the left X point. The binding energy of DP is ~ -0.14 eV, as highlighted by the blue curve. (j) EDC plot of (a) to demonstrate the existence of band anti-crossing and bulk band gap. A shoulder on the outer hole band is resolved and highlighted by a black curve. Blue dots in (g), (i), and (j) are extracted peak positions, serving as guides to the eye.

resolved photoemission spectroscopy (ARPES) studies on this series of compounds^{29,49–52} stimulated by previous investigations on LaSb⁵³, the experimental data and understandings are still ambiguous to fully determine the existence of nontrivial band topology in other compounds of the LnX family.

In this paper, we report systematic ARPES measurements and first-principles calculations on LaBi single crystals. We identify two hole-like Fermi surfaces (FSs) at the Brillouin zone (BZ) center Γ and one electron-like FS at the BZ boundary X, similar to that of LaSb. Furthermore, we find that LaBi exhibits a clear nontrivial band anti-crossing along the Γ -X direction, with the presence of one massless and one gapped Dirac-like SSs around X and Γ , respectively. Based on the observation of band inversion and odd number of massless Dirac cones, our results unambiguously demonstrate the Z_2 -type nontrivial band topology of LaBi. The diverse topological phases among the LnX series of compounds provide an excellent platform for exploring novel topological states and investigating their evolution from the perspective of TPT.

Single crystals of LaBi were grown by the Bi flux method. The residual resistance ratio [$\text{RRR} = R(300 \text{ K})/R(2 \text{ K}) = 204$] and large magnetoresistance ($\text{MR} = 3.8 \times 10^4 \%$ at 2 K under 14 T magnetic field) indicate the high quality of samples used in this work²⁴. The Vienna *ab initio* simulation package (VASP) is employed for most of the first-principles calculations. The generalized gradient approx-

imation (GGA) of Perdew-Burke-Ernzerhof (PBE) type is used for the exchange-correlation potential⁵⁴. Spin-orbit coupling is taken into account. The k -point grid in the self-consistent process is $11 \times 11 \times 11$. To get the tight-binding (TB) model Hamiltonian, we use the package wannier90 to obtain Maximally-Localized Wannier Functions (MLWFs) of d and f orbits of La and p orbit of Bi. ARPES measurements were performed at the Dreamline beamline of the Shanghai Synchrotron Radiation Facility (SSRF) with a Scienta D80 analyzer, at the Surface and Interface Spectroscopy (SIS) beamline of Swiss Light Source (SLS) using a Scienta R4000 analyzer, and at the beamline 13U of the National Synchrotron Radiation Laboratory (NSRL) equipped with a Scienta R4000 analyzer. The energy and angular resolutions were set to 15 meV and 0.2° , respectively. Fresh surfaces for ARPES measurements were obtained by cleaving the samples *in situ* along the (001) plane in a vacuum better than 5×10^{-11} Torr. All data shown in this work were recorded at $T = 30$ K.

LaBi crystallizes in a NaCl-type crystal structure (face-center cubic) with space group $Fm-3m$, in which Bi is located at the face-center adjacent to La atoms, as illustrated in Fig. 1(a). The schematic bulk Brillouin zone (BZ) and the (001)-projected 2D surface BZ are presented in Fig. 1(b). One bulk X and two bulk L points are projected to the surface $\bar{\Gamma}$ and \bar{M} points, respectively; two bulk X points are projected to the surface \bar{X} point. Figure 1(c) demonstrates the FS topologies

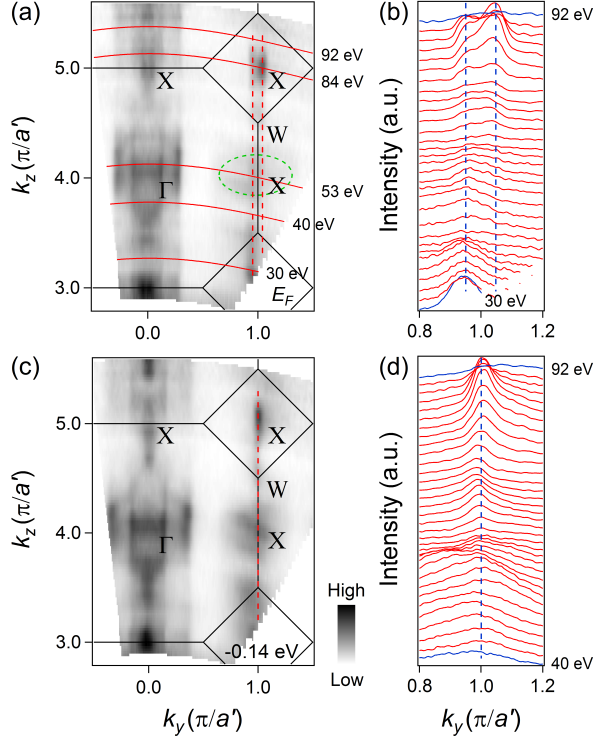


FIG. 3: (Color online) Photon energy dependence of the band structure along the Γ -X direction of LaBi. (a) Photoemission intensity plot at E_F in the k_y - k_z plane at $k_x = 0$ measured with photon energies from 20 to 100 eV. Red curves from bottom to top indicate the momentum locations taken at $h\nu = 30, 40, 53, 84$, and 92 eV, respectively. The inner potential is estimated to be 14 eV. Green dashed ellipse represents the electron-like FS at X. (b) MDC plot of (a) around the BZ boundary. (c) Same as (a) but at $E = -0.14$ eV, the binding energy of the DP at X. (d) MDC plot of (c) around the BZ boundary. Red and blue dashed lines in (a),(b) and (c),(d) demonstrate the k_z -independence of the Fermi crossings and DP of the SS around X, respectively.

of LaBi recorded with photon energy $h\nu = 84$ eV, close to the $k_z = \pi$ plane according to our photon-energy dependent study discussed below. One can obtain remarkable consistency between the experimental FSs and theoretical calculations with the PBE functional⁵⁵, as shown in Fig. 1(d), including one elliptical electron pocket at X elongated along the Γ -X direction, and two hole pockets centered at Γ with the intersecting-elliptical one enclosing the circular one. Further examining the measured FSs carefully, we can observe additional FSs around X perpendicular to the elongated pocket along the Γ -X direction, which is a common feature in the LnX series of compounds, this could be possibly interpreted by the band folding effect as a consequence of breaking translational symmetry from bulk to (001) surface⁵³. Moreover, the k_z broadening effect caused by the short escape length of the photoelectrons excited by the vacuum ultraviolet light in our ARPES experiments may also be an alternative explanation^{49,56–58}.

In order to illuminate the underlying topological properties of the measured electronic structure of LaBi, we have investi-

gated the near- E_F band dispersions along the high-symmetry lines Γ -X and X-W-X, with photon energies $h\nu = 53$ and 84 eV, close to the $k_z = 0$ and π planes, respectively. Figures 2(a) and 2(b) show the measured band structure and corresponding second derivative intensity plot along the Γ -X direction recorded with $h\nu = 53$ eV, respectively. The overall bulk band dispersions are similar to our previous study on LaSb⁵³, except that the outer hole band around Γ exhibits a shoulder at ~ -0.33 eV when gradually leveling off from Γ to X. Additionally, unlike the full parabolic electron band centered at X in LaSb, the one in LaBi curves upward towards X around the shoulder, forming a hole band with a top at ~ -0.14 eV at X. The calculated band structure using the PBE functional can reproduce these bulk features very well and indicate that LaBi is a topologically nontrivial material with band anti-crossing along the Γ -X direction⁵⁵. Using the detailed energy distribution curve (EDC) analysis presented in Fig. 2(j), we clearly observe a band gap around the shoulder, further demonstrating the existence of nontrivial band inversion in LaBi. More ARPES spectra showing much clearer features around the shoulder and the electron band centered at X measured on another piece of sample can be found in the Supplemental Material⁵⁹.

Besides the expected bulk bands, there are some additional Dirac-like surface bands around the Γ and X points. To avoid the complexity introduced by the convoluted bulk states, we investigate the electronic structure along the X-W-X direction with $h\nu = 53$ and 84 eV in Figs. 2(c)-2(i). Owing to the projection over a wide range of k_z ⁴⁹, the Dirac-like surface band around the bulk Γ point in the $k_z = 0$ (π) plane is projected to the bulk X point in the $k_z = \pi$ (0) plane, further validated by the surrounding two dispersive hole bands around the right X points in Figs. 2(c)-2(f), which are the contribution from the bulk Γ point. Thus the surface bands located at Γ points in Figs. 2(a) and 2(b) are identical to that around the right X points in Figs. 2(c)-2(f). Accordingly, it seems that the total number of Dirac points (DPs) below E_F is even, *i.e.*, two, which is inconsistent with the odd number of band anti-crossings in LaBi.

To examine this topological characteristic, we perform EDC and momentum distribution curve (MDC) studies around the right and left X points in Fig. 2(e), and present the results in Figs. 2(g) and 2(i), respectively. Unlike the massless Dirac-like surface band with a DP at ~ -0.14 eV in Fig. 2(i) (See detailed EDC plot in the Supplemental Material⁵⁹), which coincides with the valence band maximum at the X points in Figs. 2(a) and 2(b), we clearly resolve an energy gap in Fig. 2(g) separating the upper and lower linearly dispersive bands. Correspondingly, as seen in Fig. 2(h), the EDC at the right X point in Fig. 2(e) exhibits a shoulder beside the prominent peak. We use two Lorentzian curves to fit this single EDC and the fitting result is shown as the superimposed blue curve. By extracting the peak positions of Lorentzian curves, we can obtain a surface band gap of ~ 23 meV, suggesting the existence of a massive Dirac cone at the bulk Γ point. This exotic mass acquisition of Dirac fermions in LaBi was also observed recently by Wu *et al.*⁵⁰, demonstrating the novelty and complexity of the topological properties in this compound. Since the SS at Γ is proved to be gapped, the total

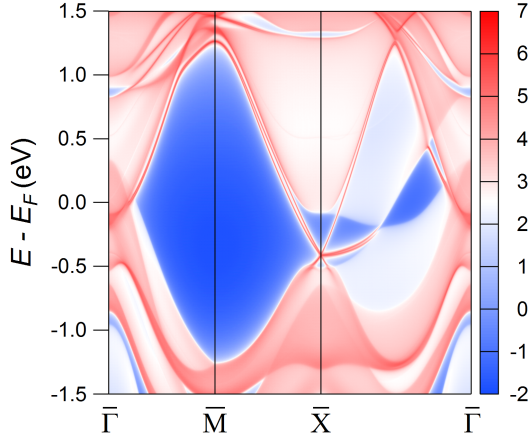


FIG. 4: (Color online) Calculated band structure along $\bar{\Gamma}$ - \bar{M} - \bar{X} - $\bar{\Gamma}$ for a semi-infinite slab of LaBi. The sharp red curves represent the SSs for (001) surface, whereas the shaded regions show the spectral weight of projected bulk bands.

number of massless Dirac cones below E_F is odd. Therefore, by summarizing the bulk and surface band dispersions along the high-symmetry lines, we conclude that LaBi is analogous to the time-reversal Z_2 nontrivial TI^{60,61}, while the massive Dirac fermion at Γ leaves an elusive issue in understanding the novel topological characteristics in LaBi.

The detailed photon-energy dependent study summarized in Fig. 3 is performed from 20 to 100 eV to demonstrate the 2D nature of the SSs. We show the FS mapping data in the k_y - k_z plane at E_F and $E = -0.14$ eV, corresponding to the DP at X , with different photon energies in Figs. 3(a) and 3(c), respectively. According to the photon energy dependence measurements, we estimate the inner potential of LaBi to 14 eV. The $k_z = 0$ and π planes at the BZ center correspond to $h\nu = 51$ and 82 eV, respectively, while at the BZ boundary the values are $h\nu = 53$ and 84 eV, respectively. As illustrated in Fig. 3(a), the two selected photon energies ($h\nu = 53$ and 84 eV) for the investigations on the electronic structure at $k_z \sim 0$ and π planes, respectively, are reasonable. We can clearly identify the two SSs around the Γ and X points showing no obvious dispersion along the k_z direction from the k_y - k_z maps in Figs. 3(a) and 3(c). We focus on the massless Dirac-like SS around X and plot the MDCs at E_F and $E = -0.14$ eV in Figs. 3(b) and 3(d), respectively. The k_z -independence of the Fermi crossings and DP provide further proof for the 2D surface band nature of this SS.

We also calculate the (001) surface band structure for a semi-infinite slab along the z direction by using Green function method, which is based on the TB Hamiltonian. As shown in Fig. 4, although one cannot unambiguously determine the SSs around $\bar{\Gamma}$ due to the convoluted bulk states, the Dirac-like SS around \bar{X} are consistent with our experimental results. The additional surface bands should relate to the topo-

logically trivial origin.

We notice that there are two recent ARPES studies focusing on the surface band structure and topological properties of LaBi^{49,51}, both reporting the presence of two separated Dirac cones at X . Nevertheless, the good consistency between our experimental band dispersions and slab model calculations demonstrate the existence of only one Dirac cone at X . Further, we perform a similar semi-infinite slab calculation terminated by the surface on the other side of cleavage, and present the result into the Supplemental Material⁵⁹. One can resolve two well separated Dirac cones located at \bar{X} from this surface termination. Although both sides of the cleavage should have identical atomic arrangement, the different calculated surface band structures make this issue much more controversial⁶². Therefore, we speculate that the distinct observations at X might result from the different surface terminations and periodic potentials after cleavage. We believe that further studies should be invested on the topological characteristics of LaBi both theoretically and experimentally.

To conclude, we have performed ARPES experiments and first-principles calculations to investigate the electronic structure and intrinsic topological characteristics of LaBi. A non-trivial band anti-crossing is obviously observed along the Γ - X direction. We further identify two distinct topological SSs. One is gapless around X and the other is massive around Γ with a ~ 23 meV gap. Such an exotic mass acquisition of Dirac fermions requires future studies to clarify. Developed theoretical calculations need to be formulated to resolve the surface band at Γ from the convoluted bulk states. The presence of band inversion and odd number of massless Dirac cones provide compelling evidence that LaBi is analogous to the time-reversal Z_2 TI. The rich and novel topological states in LaBi and other compounds of the LnX family offer an excellent opportunity for investigating the evolution of topological properties from the perspective of TPT, facilitating the future search of new topological phases.

This work was supported by the Ministry of Science and Technology of China (Programs No. 2012CB921701, No. 2013CB921700, No. 2015CB921000, No. 2016YFA0300300, No. 2016YFA0300504, No. 2016YFA0300600, No. 2016YFA0302400, and No. 2016YFA0401000), the National Natural Science Foundation of China (Grants No. 11274381, No. 11274362, No. 11474340, No. 11234014, No. 11274367, No. 11474330, No. 11574394, and No. 11674371), and the Chinese Academy of Sciences (CAS) (Project No. XDB07000000). RL and KL were supported by the Fundamental Research Funds for the Central Universities, and the Research Funds of Renmin University of China (RUC) (Grants No. 17XNH055, No. 14XNLQ03, No. 15XNLF06, and No. 15XNLQ07). Computational resources have been provided by the Physical Laboratory of High Performance Computing at RUC. The FSs were prepared with the XCRYSDEN program⁶³. YH was supported by the CAS Pioneer Hundred Talents Program.

* Electronic address: scw@ruc.edu.cn

¹ M. Z. Hasan and C. L. Kane, Rev. Mod. Phys. **82**, 3045 (2010).

- ² X. L. Qi and S. C. Zhang, *Rev. Mod. Phys.* **83**, 1057 (2011).
- ³ H. Weng, X. Dai, and Z. Fang, *MRS Bulletin* **39**, 849 (2014).
- ⁴ C. L. Kane and E. J. Mele, *Phys. Rev. Lett.* **95**, 226801 (2005).
- ⁵ B. A. Bernevig, T. L. Hughes, and S. C. Zhang, *Science* **314**, 1757 (2006).
- ⁶ M. König, S. Wiedmann, C. Brüne, A. Roth, H. Buhmann, L. W. Molenkamp, X.-L. Qi, and S.-C. Zhang, *Science* **318**, 766 (2007).
- ⁷ I. Knez, R.-R. Du, and G. Sullivan, *Phys. Rev. Lett.* **107**, 136603 (2011).
- ⁸ Y. L. Chen, J. G. Analytis, J.-H. Chu, Z. K. Liu, S.-K. Mo, X. L. Qi, H. J. Zhang, D. H. Lu, X. Dai, Z. Fang, S. C. Zhang, I. R. Fisher, Z. Hussain, and Z.-X. Shen, *Science* **325**, 178 (2009).
- ⁹ A. A. Burkov, M. D. Hook, and L. Balents, *Phys. Rev. B* **84**, 235126 (2011).
- ¹⁰ R. Yu, H. M. Weng, Z. Fang, X. Dai, and X. Hu, *Phys. Rev. Lett.* **115**, 036807 (2015).
- ¹¹ L. Fu, *Phys. Rev. Lett.* **106**, 106802 (2011).
- ¹² T. H. Hsieh, H. Lin, J. Liu, W. Duan, A. Bansil, and L. Fu, *Nat. Commun.* **3**, 982 (2012).
- ¹³ Z. Wang, Y. Sun, X.-Q. Chen, C. Franchini, G. Xu, H. Weng, X. Dai, and Z. Fang, *Phys. Rev. B* **85**, 195320 (2012).
- ¹⁴ Z. K. Liu, B. Zhou, Y. Zhang, Z. J. Wang, H. Weng, D. Prabhakaran, S.-K. Mo, Z. X. Shen, Z. Fang, X. Dai, Z. Hussain, and Y. L. Chen, *Science* **343**, 864 (2014).
- ¹⁵ H. Weng, C. Fang, Z. Fang, B. A. Bernevig, and X. Dai, *Phys. Rev. X* **5**, 011029 (2015).
- ¹⁶ B. Q. Lv, H. M. Weng, B. B. Fu, X. P. Wang, H. Miao, J. Ma, P. Richard, X. C. Huang, L. X. Zhao, G. F. Chen, Z. Fang, X. Dai, T. Qian, and H. Ding, *Phys. Rev. X* **5**, 031013 (2015).
- ¹⁷ S. Huang, S. Xu, I. Belopolski, C. Lee, G. Chang, B. Wang, N. Alidoust, G. Bian, M. Neupane, C. Zhang, S. Jia, A. Bansil, H. Lin, and M. Z. Hasan, *Nat. Commun.* **6**, 7373 (2015).
- ¹⁸ S. Xu, I. Belopolski, N. Alidoust, Madhab Neupane, G. Bian, C. Zhang, R. Sankar, G. Chang, Z. Yuan, C. Lee, S. Huang, H. Zheng, J. Ma, D. S. Sanchez, B. Wang, A. Bansil, F. Chou, P. P. Shibaev, H. Lin, S. Jia, and M. Z. Hasan, *Science* **349**, 613 (2015).
- ¹⁹ Y. Ando, *J. Phys. Soc. Jpn.* **82**, 102001 (2013).
- ²⁰ T. Sato, K. Segawa, K. Kosaka, S. Souma, K. Nakayama, K. Eto, T. Minami, Y. Ando, and T. Takahashi, *Nat. Phys.* **7**, 840 (2011).
- ²¹ S. Xu, Y. Xia, L. Wray, S. Jia, F. Meier, J. H. Dil, J. Osterwalder, B. Slomski, A. Bansil, H. Lin, R. J. Cava, and M. Z. Hasan, *Science* **332**, 560 (2011).
- ²² R. Lou, Z.-H. Liu, W.-C. Jin, H. F. Wang, Z. Q. Han, K. Liu, X.-Y. Wang, T. Qian, Y. Kushnirenko, S.-W. Cheong, R. M. Osgood, H. Ding, and S.-C. Wang, *Phys. Rev. B* **92**, 115150 (2015).
- ²³ F. F. Tafti, Q. D. Gibson, S. K. Kushwaha, N. Haldolaarachchige, and R. J. Cava, *Nat. Phys.* **12**, 272 (2015).
- ²⁴ S. S. Sun, Q. Wang, P. J. Guo, K. Liu, and H. C. Lei, *New J. Phys.* **18**, 082002 (2016).
- ²⁵ N. Kumar, C. Shekhar, S.-C. Wu, I. Leermakers, O. Young, U. Zeitler, B. H. Yan, and C. Felser, *Phys. Rev. B* **93**, 241106(R) (2016).
- ²⁶ Q. Yu, Y. Wang, S. Xu, and T.-L. Xia, *arXiv:1604.05912*.
- ²⁷ O. Pavlosiuk, P. Swatek, and P. Wiśniewski, *arXiv:1604.06945*.
- ²⁸ N. Wakeham, E. D. Bauer, M. Neupane, and F. Ronning, *Phys. Rev. B* **93**, 205152 (2016).
- ²⁹ N. Alidoust, A. Alexandradinata, S.-Y. Xu, I. Belopolski, S. K. Kushwaha, M. Zeng, M. Neupane, G. Bian, C. Liu, D. S. Sanchez, P. P. Shibaev, H. Zheng, L. Fu, A. Bansil, H. Lin, R. J. Cava, and M. Z. Hasan, *arXiv:1604.08571*.
- ³⁰ M. Zeng, C. Fang, G. Chang, Y.-A. Chen, T. Hsieh, A. Bansil, H. Lin, and L. Fu, *arXiv:1504.03492*.
- ³¹ K. Wang, D. Graf, L. Li, L. Wang, and C. Petrovic, *Sci. Rep.* **4**, 7328 (2014).
- ³² B. Shen, X. Y. Deng, G. Kotliar, and N. Ni, *Phys. Rev. B* **93**, 195119 (2016).
- ³³ D. S. Wu, J. Liao, W. Yi, X. Wang, P. G. Li, H. M. Weng, Y. G. Shi, Y. Q. Li, J. L. Luo, X. Dai, and Z. Fang, *Appl. Phys. Lett.* **108**, 042105 (2016).
- ³⁴ C. C. Xu, J. Chen, G. X. Zhi, Y. K. Li, J. H. Dai, and C. Cao, *Phys. Rev. B* **93**, 195106 (2016).
- ³⁵ Y.-Y. Wang, Q.-H. Yu, P.-J. Guo, K. Liu, and T.-L. Xia, *Phys. Rev. B* **94**, 041103(R) (2016).
- ³⁶ Z. Wang, Y. Li, Y. Lu, Z. Shen, F. Sheng, C. Feng, Y. Zheng, and Z. A. Xu, *arXiv:1603.01717*.
- ³⁷ R. Singha, A. Pariari, B. Satpati, and P. Mandal, *arXiv:1602.01993*.
- ³⁸ M. N. Ali, L. M. Schoop, C. Garg, J. M. Lippmann, E. Lara, B. Lotsch, and S. Parkin, *arXiv:1603.09318*.
- ³⁹ X. F. Wang, X. C. Pan, M. Gao, J. H. Yu, J. Jiang, J. R. Zhang, H. K. Zuo, M. H. Zhang, Z. X. Wei, W. Niu, Z. C. Xia, X. G. Wan, Y. L. Chen, F. Q. Song, Y. B. Xu, B. G. Wang, G. H. Wang, and R. Zhang, *Adv. Electron. Mater.* **2**, 1600228 (2016).
- ⁴⁰ M. N. Ali, J. Xiong, S. Flynn, J. Tao, Q. D. Gibson, L. M. Schoop, T. Liang, N. Haldolaarachchige, M. Hirschberger, N. P. Ong, and R. J. Cava, *Nature (London)* **514**, 205 (2014).
- ⁴¹ J. Feng, Y. Pang, D. Wu, Z. Wang, H. Weng, J. Li, X. Dai, Z. Fang, Y. Shi, and L. Lu, *Phys. Rev. B* **92**, 081306 (2015).
- ⁴² T. Liang, Q. Gibson, M. N. Ali, M. Liu, R. J. Cava, and N. P. Ong, *Nat. Mater.* **14**, 280 (2015).
- ⁴³ X. C. Huang, L. X. Zhao, Y. J. Long, P. P. Wang, D. Chen, Z. H. Yang, H. Liang, M. Q. Xue, H. M. Weng, Z. Fang, X. Dai, and G. F. Chen, *Phys. Rev. X* **5**, 031023 (2015).
- ⁴⁴ C. Shekhar, A. K. Nayak, Y. Sun, M. Schmidt, M. Nicklas, I. Leermakers, U. Zeitler, Z. K. Liu, Y. L. Chen, W. Schnelle, J. Grin, C. Felser, and B. H. Yan, *Nat. Phys.* **11**, 645 (2015).
- ⁴⁵ J. Jiang, F. Tang, X. C. Pan, H. M. Liu, X. H. Niu, Y. X. Wang, D. F. Xu, H. F. Yang, B. P. Xie, F. Q. Song, P. Dudin, T. K. Kim, M. Hoesch, P. K. Das, I. Vobornik, X. G. Wan, and D. L. Feng, *Phys. Rev. Lett.* **115**, 166601 (2015).
- ⁴⁶ I. Pletikosić, M. N. Ali, A. V. Fedorov, R. J. Cava, and T. Valla, *Phys. Rev. Lett.* **113**, 216601 (2014).
- ⁴⁷ L. M. Schoop, M. N. Ali, C. Straßer, V. Duppel, S. S. P. Parkin, B. V. Lotsch, and C. R. Ast, *Nat. Commun.* **7**, 11696 (2016).
- ⁴⁸ R. Lou, J.-Z. Ma, Q.-N. Xu, B.-B. Fu, L.-Y. Kong, Y.-G. Shi, P. Richard, H.-M. Weng, Z. Fang, S.-S. Sun, Q. Wang, H.-C. Lei, T. Qian, H. Ding, and S.-C. Wang, *Phys. Rev. B* **93**, 241104(R) (2016).
- ⁴⁹ X. H. Niu, D. F. Xu, Y. H. Bai, Q. Song, X. P. Shen, B. P. Xie, Z. Sun, Y. B. Huang, D. C. Peets, and D. L. Feng, *Phys. Rev. B* **94**, 165163 (2016).
- ⁵⁰ Y. Wu, T. Kong, L.-L. Wang, D. D. Johnson, D. Mou, L. Huang, B. Schtrunk, S. L. Bud'ko, P. C. Canfield, and A. Kaminski, *Phys. Rev. B* **94**, 081108(R) (2016).
- ⁵¹ J. Nayak, S.-C. Wu, N. Kumar, C. Shekhar, S. Singh, J. Fink, E. E. D. Rienks, G. H. Fecher, S. S. P. Parkin, B. Yan, and C. Felser, *arXiv:1605.06997*.
- ⁵² M. Neupane, M. M. Hosen, I. Belopolski, N. Wakeham, K. Dimitri, N. Dhakal, J.-X. Zhu, M. Z. Hasan, E. D. Bauer, and F. Ronning, *J. Phys.: Condens. Matter* **28**, 23LT02 (2016).
- ⁵³ L.-K. Zeng, R. Lou, D.-S. Wu, Q. N. Xu, P.-J. Guo, L.-Y. Kong, Y.-G. Zhong, J.-Z. Ma, B.-B. Fu, P. Richard, P. Wang, G. T. Liu, L. Lu, Y.-B. Huang, C. Fang, S.-S. Sun, Q. Wang, L. Wang, Y.-G. Shi, H. M. Weng, H.-C. Lei, K. Liu, S.-C. Wang, T. Qian, J.-L. Luo, and H. Ding, *Phys. Rev. Lett.* **117**, 127204 (2016).
- ⁵⁴ J. P. Perdew, K. Burke, and M. Ernzerhof, *Phys. Rev. Lett.* **77**, 3865 (1996); **78**, 1396 (1997).

- ⁵⁵ P.-J. Guo, H.-C. Yang, B.-J. Zhang, K. Liu, and Z.-Y. Lu, *Phys. Rev. B* **93**, 235142 (2016).
- ⁵⁶ H. Kumigashira, H.-D. Kim, A. Ashihara, A. Chainani, T. Yokoya, T. Takahashi, A. Uesawa, and T. Suzuki, *Phys. Rev. B* **56**, 13654 (1997).
- ⁵⁷ H. Kumigashira, H.-D. Kim, T. Ito, A. Ashihara, T. Takahashi, T. Suzuki, M. Nishimura, O. Sakai, Y. Kaneta, and H. Harima, *Phys. Rev. B* **58**, 7675 (1998).
- ⁵⁸ V. N. Strocov, *J. Electron Spectrosc. Relat. Phenom.* **130**, 65 (2003).
- ⁵⁹ See Supplemental Material for clearer ARPES spectra around the shoulder and the electron band centered at X, EDC plot of Fig. 2(e) around the left X point, and the semi-infinite slab calculation terminated by the surface on the other side of cleavage.
- ⁶⁰ J. E. Moore and L. Balents, *Phys. Rev. B* **75**, 121306(R) (2007).
- ⁶¹ L. Fu, C. L. Kane, and E. J. Mele, *Phys. Rev. Lett.* **98**, 106803 (2007).
- ⁶² S.-Y. Xu, N. Alidoust, I. Belopolski, Z. Yuan, G. Bian, T.-R. Chang, H. Zheng, V. N. Strocov, D. S. Sanchez, G. Chang, C. Zhang, D. Mou, Y. Wu, L. Huang, C.-C. Lee, S.-M. Huang, B. Wang, A. Bansil, H.-T. Jeng, T. Neupert, A. Kaminski, H. Lin, S. Jia, and M. Z. Hasan, *Nat. Phys.* **11**, 748 (2015).
- ⁶³ A. Kokalj, *Comput. Mater. Sci.* **28**, 155 (2003).